THE EFFECT OF TARGET TOPOGRAPHY AND IMPACT ANGLE ON CRATER FORMATION - INSIGHT FROM 3D NUMERICAL MODELLING.

Dirk Elbeshausen[1,+] and Kai Wünnemann[1]
[1]Museum für Naturkunde, Leibniz-Institut an der Humboldt-Universität zu Berlin, Invalidenstr. 43, D-10115 Berlin, Germany, [+]email: dirk.elbeshausen@mfn-berlin.de

Introduction: Although nearly every meteorite impact occurs at an oblique angle of incidence [1], most of our knowledge of impact cratering is inferred from vertical laboratory experiments and two-dimensional (2D) axis-symmetric numerical modeling only.

Laboratory impact experiments are inevitable for understanding impact cratering. However, only very few of them have been carried out under an oblique angle of incidence [e.g. 2-5]. Such experiments are limited by the range of material properties of the target (yield strength, friction, porosity) but most importantly by the small scale in comparison to the dimensions of natural impact craters. Therefore the effect of gravity on crater growth and subsequent collapse is difficult to investigate experimentally. A number of three-dimensional (3D) computer simulations have been carried out to study how the impact angle affects crater efficiency [6-8], the propagation of shock waves [9], the generation and distribution of impact melt [10], the expansion of the ejecta plume [11], and the crater collapse [12,13]. However, due to the high computational costs no large parameter study has been performed.

It is still a matter of debate whether asymmetries found in impact structures are due to an oblique angle of incidence or caused by target heterogeneities [14]. So far, the effect of topography has neither been studied in an experimental nor in an numerical framework. Here we present results of a comprehensive study comprising more than 1000 3D hydrocode simulations. The study gives insight into the effect of the impact angle and target topography on the morphometry and morphology of impact structures as well as their formation processes. The calculations have been carried out with the multi-rheology hydrocode iSALE-3D [6,15] which considers a strength-model for rock [16] and acoustic fluidization [17].

Crater shape and distribution of ejecta: Fig. 1 illustrates that the overall shape of the resulting crater for impacts at angles between 90° (vertical) and 30° remains circular in plane. Our models show that for constant impact energy and decreasing impact angle (1) the height of the central peak decreases, (2) the position of the central peak is slightly offset downrange, and (3) the time of central peak formation decreases in a sinusoidal manner. Generally our results agree with [12], but our study covers a much broader parameter range and a larger number of simulations and, thus, allows for a more precise interpretation of central peak formation.

The ejecta blanket shows a characteristic pattern (e.g. an emerging 'forbidden zone' in uprange-direction) that can be easily linked to the direction of impact. However, the ejecta-blanket is often not well preserved and, hence, not available as an indicator for the impact angle.

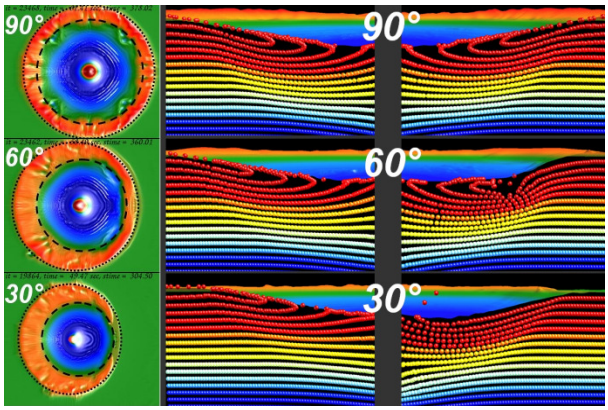

Figure 1 Influence of the impact angle on crater shape and stratigraphy. Left: Topview into the final crater; Right: Post-Impact stratigraphy below the crater rim downrange (left) and uprange (right).

Structural deformation and central peak formation: Most terrestrial impact structures have undergone major erosion. This raises the question whether an oblique impact produces diagnostic structural features underneath the surface that may be exposed if a crater is eroded. Our models show that at impact angles α lower than a threshold angle ($30° < \alpha_c < 60°$) no overturning of the uppermost layer in uprange direction occurs (Fig. 1, right).

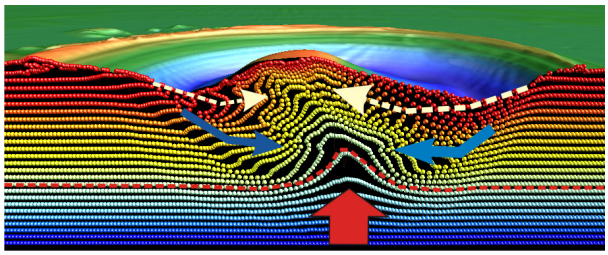

Figure 2 Peak formation by an oblique (30°) impact. Arrows indicate main material fluxes. Notice the symmetric uplift in the deeper strata.

Peak formation starts when the transient crater collapses. A strong, upward-directed material flow originates from the deepest point of the transient cavity which is located offset in uprange direction with respect to the symmetric centre of the final crater. The rise of the crater floor results in a symmetric stratigraphic uplift in the deeper region, causes sagging of the upper stratigraphic units and inward slumping of material from the oversteepend sides of the crater. The latter two processes are directed towards the crater centre, they are highly asymmetric depending on the impact angle, and they cause a slight uprange shift of the peak with respect to the geometric centre of the final crater (Fig. 2). In case of large impact craters, collapse of the central peak is more pronounced in the downrange direction.

Effect of the impact angle on crater size: Crater size decreases proportional to the sinus of the impact angle α. This decrease is more pronounced for stronger materials. The often reported assumption that only the vertical component of the impact velocity contributes to the cratering (e.g. [18]) does not hold for impacts into materials with properties significantly different to those of sand, e.g. competent rock [6].

From circular to elliptic craters: The transition from circular to elliptic craters is smooth and can be characterized by three different regimes: (i) the transition regime, (ii) the ricochet regime, and (iii) the grazing regime [22]. The impact crater is the result of both a moving point source [23] in the initial stage and a static point source from onset of the excavation stage. Depending on which of both processes dominates the other, the resulting crater is either circular or elliptic. As Fig. 3 shows, the threshold-angle for the evolution of elliptical craters is a function of cratering efficiency, regardless of the target material or cratering regime.

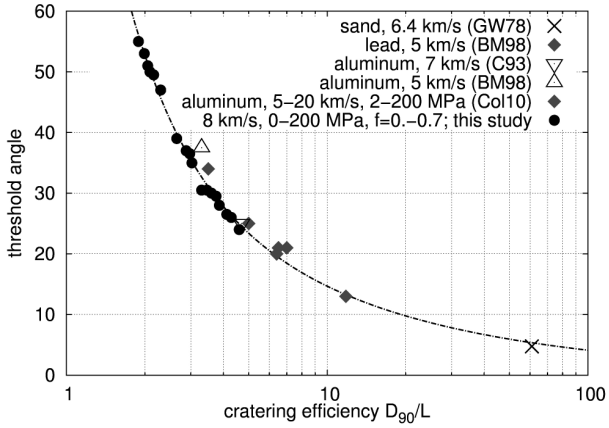

Figure 3 Threshold angle for elliptic craters vs. cratering efficiency (here: ratio between crater diameter of the vertical impact and the projectile size). This graph shows also results derived from other simulations (Col10=[19]) and laboratory experiments (GW78=[3], BM98=[20], C93=[21]) and spans both the gravity and strength-dominated regime.

Effect of topography: Our models of impacts on tilted targets with different slopes (0-90°) show that topography causes patterns in the ejecta distribution (Fig. 4) and often an asymmetric crater shape that might be diagnostic for the impact direction. Ejection angle and ejection speed increase for larger slopes. Hence, how much of the ejected material approaches the escape velocity and might leave a planet is significantly influenced by topography.

Summary and conclusion: This study revealed that both an oblique angle of incidence and pre-impact target topography affect crater morphometry and cause asymmetric structural features at and beneath impact craters. The large parameter study of 3D hydrocode simulations enables quantification of the processes and gives insight how to distinguish between structural features that are diagnostic for the impact angle and those primary caused by topography.

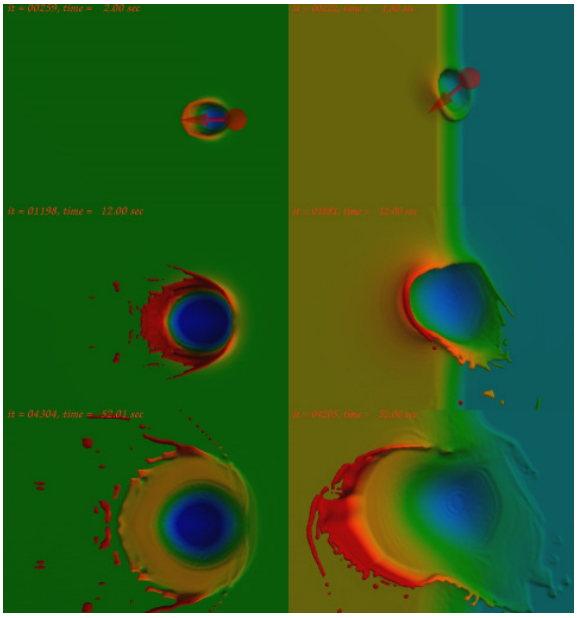

Figure 4 Snapshots of crater formation for an oblique (45°) impact in a planar target (left) and a small slope (45°, right).

Acknowledgement: This work was funded by DFG grant WU 355/5-2 and the Helmholtz-Alliance HA-203 / "Planetary Evolution and Life" by the Helmholtz-Gemeinschaft Deutscher Forschungszentren (HGF).

References: [1] Shoemaker E. M. (1962) In: *Physics and Astronomy of the Moon*, Academic Press, San Diego, 283-359. [2] Dahl J. M. and Schultz P. H. (2001) *Int. J. Imp. Engin. 26*, 145-155. [3] Gault D. E. and Wedekind J. A. (1978). *In: Proc. LPS IX*, 3843-3875. [4] Anderson J. L. B. et al. (2003) *JGR-Planets, 108,* 5094. [5] Burchell M. J. and Whitehorn L. (2003) *Mon. Not. R. Astron. Soc. 341*, 192-198. [6] Elbeshausen D. et al. (2009) *Icarus 204*, 716-731. [7] Elbeshausen D. et al. (2007) *LPS XXXVIII*, Abstract #1952. [8] Elbeshausen D. et al. (2008) *LPS XXXIX*, Abstract #1795. [9] Pierazzo E. and Melosh H. J. (2000) *MAPS 35*, 117-130. [10] Pierazzo E., Melosh H. J. (2000) *Icarus 145*, 252-261. [11] Artemieva N. A. et al. (2002) *Bull.Czech Geol.Survey 77* (4), 31-39. [12] Shuvalov V. V. (2003). *Large Met. Impacts Conf. 3rd*, Abstract #4130. [13] Ivanov B. A. and Artemieva N. A. (2002) *GSA Spec. Papers* 356, 619-630. [14] Collins G. S. et al. (2008) *EPSL, 270*, 221-230. [15] Elbeshausen D. and Wünnemann K. (2011) *Proc. HVIS XI* (in press). [16] Collins G. S. et al. (2004) *MAPS 39* (2), 217-231. [17] Wünnemann K. and Ivanov B.A. (2003). *Planet. Space Sci. 51*, 831-845. [18] Chapman C. R. and McKinnon W. B. (1986). In: *Satellites*, Univ. of Arizona Press, Tucson, pp. 492-580. [19] Collins G. S. et al. (2010) *EPSC*, Abstract #238. [20] Burchell M. J. and Mackay N. G. (1998) *JGR 103* (E10), 22761-22774. [21] Christiansen E. L. et al. (1993) *Int. J. Imp. Engin. 14*, 157-168. [22] Elbeshausen D. and Wünnemann K. (2010) *EPSC*, Abstract #73. [23] Anderson J. L. B. and Schultz P. H. (2006) *Int. J. Imp. Engin. 33*, 35-44.